Contribution from Research School of Chemistry,
Australian National University, Canberra, A.C.T., Australia

Electronic Absorption Spectra of Tetragonal and Pseudotetragonal Cobalt(II). II. $CoCl_2{\cdot}6H_2O$ and $CoCl_2{\cdot}6D_2O$

JAMES FERGUSON* and T. E. WOOD

Received April 24, 1974

AIC40273H

The electronic absorption spectra of $CoCl_2{\cdot}6H_2O$ and $CoCl_2{\cdot}6D_2O$ have been measured in polarized light and at various temperatures down to 6 K over the range 5000–45,000 cm^{-1}. From measurements made with light incident normal to three different crystal faces it has been possible to make a definitive analysis of all of the bands observed. The bands fall into three categories: (1) water overtones, (2) normal crystal field bands, and (3) anomalous crystal field bands. An analysis of the normal crystal field bands provides the following parameters: $Dq = 810 \pm 15$ cm^{-1}, $Ds = -640 \pm 15$ cm^{-1}, and $Dt = 30 \pm 10$ cm^{-1}. Electric and magnetic dipole absorption bands are present, the latter in the near-infrared region associated with the transition ${}^4A_{2g}{}^a \rightarrow {}^4E_g{}^b$. The anomalous crystal field bands involve the symmetrical OH stretching mode as a perturbing vibration which breaks down the $g \leftarrow\!|\!\rightarrow g$ selection rule.

Introduction

The two cobalt chloride hydrates $CoCl_2{\cdot}6H_2O$ and $CoCl_2{\cdot}2H_2O$ contain cobalt ions surrounded by an approximately tetragonal array of ligands. In the first, four water molecules lie in a square plane about the cobalt with the chloride ions in the axial positions, while in the second, the ligands are interchanged. Together the two crystals provide examples of related pseudotetragonal ligand fields and we have carried out quantitative studies of the crystal spectra of both materials. The present paper is concerned with the hexahydrate while the following paper[1] deals with the dihydrate.

There have been many studies of the physical properties of $CoCl_2{\cdot}6H_2O$, particularly in relation to its magnetic properties. Haseda and Kanda[2] noted that a transition to an antiferromagnetic state occurs at about 3 K. Subsequent measurements of the *g* factors provided some idea of the energy level structure of the ground state in terms of two Kramers doublets 120–150 and 630–760 cm^{-1} above the ground state.[3] The measurements of single-crystal magnetic susceptibility in the 4–30 K range were then accounted for by Kimura and Uryu.[4]

In spite of the many magnetic measurements there has been no adequate description of the overall ground state of $CoCl_2{\cdot}6H_2O$. For example, Figgis, *et al.*,[5] were unable to distinguish between a ${}^4A_{2g}$ and a ${}^4E_g$ ground state and, more recently, Gerloch, *et al.*,[6] using calculations which included all the spin quartets were nevertheless unable to determine the signs of the tetragonal field parameters.

Measurements of the absorption spectrum of $CoCl_2{\cdot}6H_2O$ have been made by Gielessen,[7] Pappalardo,[8] and Ferguson,[9] but no detailed analysis of all of the bands has been given.

Crystal Structure of $CoCl_2{\cdot}6H_2O$. The crystal structure of $CoCl_2{\cdot}6H_2O$ is known[10,11] and even the locations of the hydrogen atoms have been determined.[12] The structure contains $CoCl_2(H_2O)_4$ units with the remaining two water molecules some distance from the cobalt (Co–O = 407 pm). The four coordinated water molecules are in a plane perpendicular to (010) and inclined to *c* by about 10°, and they form an almost square array about the cobalt ion (rectangular sides 305 and 294 pm with all Co–O distances equal to 212 pm. The Cl–Co–Cl axis is perpendicular to the plane of the water molecules (Co–Cl = 243 pm).

The structure has atomic layers parallel to (001) which accounts for the perfect cleavage in the *ab* plane. No low-temperature crystal structure data have been reported, but since no anomalies have been found in either the magnetic or optical absorption studies, it is assumed that, apart from thermal contraction, the low-temperature structure is the same.

An analysis of the various crystal spectra requires a knowledge of the projections of the $CoCl_2(H_2O)_4$ unit on the *ab*, *ac'*, and *bc'* faces. These are given in Figure 1, along with the molecular axis definition. The appropriate direction cosine matrix transforms the (*a*, *b*, *c'*) crystal axes to the (*x*, *y*, *z*) molecular axes and, as the transition intensities are related to the squares of the projections of the various transition moments, polarization behavior in one coordinate system may be compared with the other using the matrix of the squares of direction cosines given in Table I. From Table I we note that the *b* and *x* axes are equivalent, while the *y* and *z* axes project principally on the *a* and *c'* directions, respectively.

Table I. Squares of Unit Vector Projections on the Crystal Axis

	Crystal axis		
$CoCl_2{\cdot}(OH_2)_4$ axis	*a*	*b*	*c'*
x	0	1	0
y	0.158	0	0.842
z	0.842	0	0.158

Experimental Section

Large single crystals of the hexahydrate were grown by recrystallization of AnalaR $CoCl_2{\cdot}6H_2O$ from aqueous solution at room temperature. Crystals of the hexadeuterate were obtained in a similar way from a solution prepared from anhydrous cobalt chloride (obtained by thermal dehydration of the hexahydrate) dissolved in D_2O (99.75%). To prevent exchange with atmospheric water, crystallization was carried out inside a glove bag, periodically flushed with dry nitrogen.

As the hexahydrate is a biaxial crystal, two polarized spectra are required for light incident on each of three orthogonal faces.[13] The crystals cleave perfectly in the *ab* plane so this together with *ac'* and *bc'*, obtained by sectioning perpendicular to the plane along *a* and *b*, were used for the spectral measurements. Extinction directions in *ac'* are not fixed by the crystal symmetry but they were found, for visible light, to lie along *a* and *c*. These directions were used for the near-infrared region with the assumption that there is no significant wavelength dispersion.

All absorption measurements were recorded with a Cary 17 spectrophotometer and matched Glan-Taylor polarizers were used in the sample and reference compartments. Cooling of the samples was achieved by thermal exchange with controlled boil-off from a liquid helium storage vessel placed below the sample compartment, passing over the crystal in a silica flow tube. Control of the gas flow rate enabled steady temperatures from 6 to 300 K to be obtained. $CoCl_2{\cdot}6H_2O$ will immediately dehydrate in the stream of cold helium gas unless the crystal is protected. Two methods were used with success. The first involves coating the crystal with rubber cement and this is a simple procedure for work in the visible and infrared spectral regions. The second, more elaborate method was used for measurements in the ultraviolet. It involved sealing the sample, plus some loose crystals and helium gas, in a square cross section silica tube.

Raman scattering experiments were performed with 647.1-nm radiation from a krypton laser and a Spex double monochromator using photon counting. The samples were cooled to 30–40 K by means of cold helium gas in a silica flow tube. Since one extinction direction

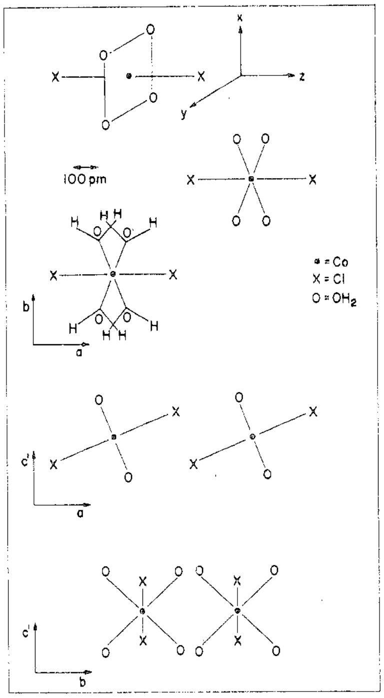

Figure 1. Cobalt chloride hexahydrate. Projections of $[CoCl_2 \cdot 4H_2O]$ on *ab*, *ac'*, and *bc'* crystal faces.

always lies along the unique (*b*) axis, the directions perpendicular to the *ab* and *bc'* faces were used for light propagation (see Gilson and Hendra).[14] The single-crystal samples were sealed into glass capillaries to prevent dehydration by the stream of helium gas.

Results and Discussion

Gross Spectral Features. Polarized absorption spectra were measured from about 5000 to about 45,000 cm^{-1}, which is the ultraviolet absorption edge. The near-infrared region records some broad bands as well as very sharp lines, as narrow as a few reciprocal centimeters at low temperatures. These latter lines are easily assigned to overtones of water vibrations, particularly from their behavior on deuteration. Figure 2 shows a typical result and spectra of the hexadeuterate were measured for all crystal faces to identify the absorption due to H_2O and D_2O. These absorption lines have been subtracted from subsequent spectra reported here.

The remaining absorption bands are broader and they fall into two groups, one normal and the other anomalous. The normal group contains typical vibronic bands which decrease in absorption intensity on cooling the crystals. In the visible region these bands are electric dipole in origin, whereas in the infrared region an examination of the six polarized spectra shows that there is considerable magnetic dipole character present and this region will be discussed separately. The anomalous group comprises mainly two broad bands, one near 11,500 cm^{-1} and the other near 25,800 cm^{-1}, which are polarized in the molecular plane parallel to the *x* axis and increase in absorption intensity on cooling the crystals.

The Near-Infrared Region. The electronic transition from $^4T_{1g}(^4F)$ to $^4T_{2g}(^4F)$ is allowed for magnetic dipole absorption of radiation and the need to measure six sets of spectra is demonstrated in Figure 3 for the 7000–10,000-cm^{-1} region. The band positions and intensities are collected in Table II. Bearing in mind that there are six possible contributions to the absorption intensities, e_i and m_i with $i = a, b, c'$, the data in Table II allow us to fix approximate ranges for the magnetic (m_i) and electric dipole (e_i) oscillator strengths (in units of 10^{-6}) in the following way: $m_a = 0$–2, $m_b \approx m_{c'} = 3$–5, $e_a = 7.5$–9.5, $e_b \approx e_{c'} = 0.2$.

In spite of the crudeness of these estimates it appears that there are major contributions from a *bc'*(*xy*)-polarized magnetic dipole transition and an *a*(*z*)-polarized electric dipole (vibronic) band. This conclusion is supported by the temperature dependences of the intensities listed in Table II, which show clearly that the bands which have the greatest magnetic dipole character have the least temperature dependence.

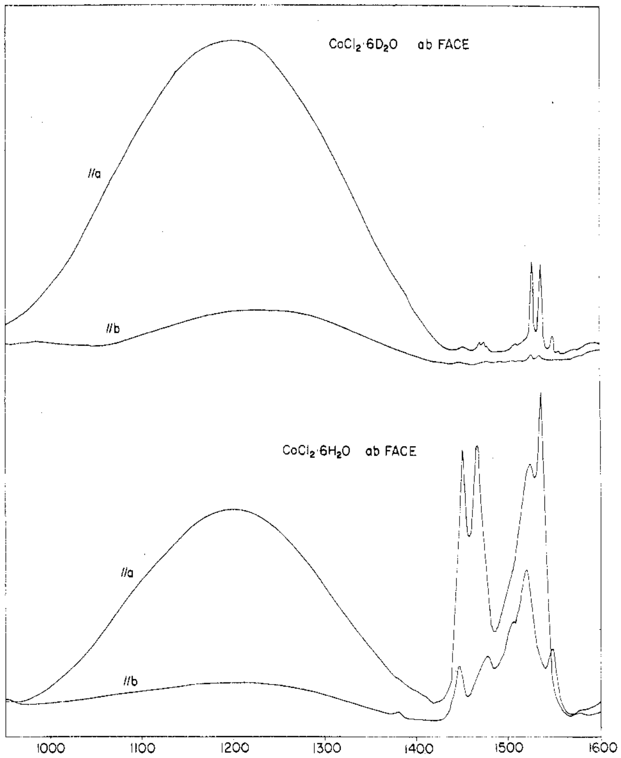

Figure 2. H_2O–D_2O vibrational overtones. Polarized absorption spectra of *ab* faces of $CoCl_2 \cdot 6H_2O$ (45 K) and $CoCl_2 \cdot 6D_2O$ (16 K).

Table II. Infrared Bands in $CoCl_2 \cdot 6H_2O$ and $CoCl_2 \cdot 6D_2O$

Polarizn[a]	Position[b]	f_{10}[c]	f_{300}/f_{10}
ab∥*a*	8330 ± 30	12.5	2.0
ac'∥*a*	8330 ± 50	12.5	2.0
ab∥*b*	8065 ± 60	2.5	1.7
bc'∥*b*	8160 ± 60	5.5	1.1
ac'∥*c'*	8200 ± 50	2.0	1.6
bc'∥*c'*	8200 ± 60	5.0	1.1

[a] Crystal face and polarization of electric vector. [b] Franck–Condon maxima at 10 K (cm^{-1}). [c] Units of 10^{-6}. Larger values ±10%, smaller values ±20%.

A search was made for magnetic dipole zero phonon lines in the low-energy tail of the absorption region. This region is confused by the water overtones but from measurements made with the hydrate and the deuterate, the presence of three lines was established. The data are shown in Figure 4. The lines are very weak and it is possible that the lines are sharper than is shown in Figure 4. An examination of the spectra shows that the lines at 7092 ± 2 and 7018 ± 2 cm^{-1} ($CoCl_2 \cdot 6H_2O$) and 7122 ± 5 and 7052 ± 5 cm^{-1} ($CoCl_2 \cdot 6D_2O$) are magnetic dipole in character, with the active direction in the *bc'* plane, in agreement with the conclusion reached in the previous paragraph.

We can reasonably conclude therefore that the absorption region near 8000 cm^{-1} is associated with two broad superimposed bands, one arising through a vibronic (electric dipole) mechanism and strongly polarized in the *z* direction and the other through a magnetic dipole mechanism, polarized in the *xy* plane. Careful examination of the positions of the various Franck–Condon maxima reveals that this conclusion is also consistent with the observed splittings. The magnetic dipole transition has its band maximum close to 8060 ± 60 cm^{-1}

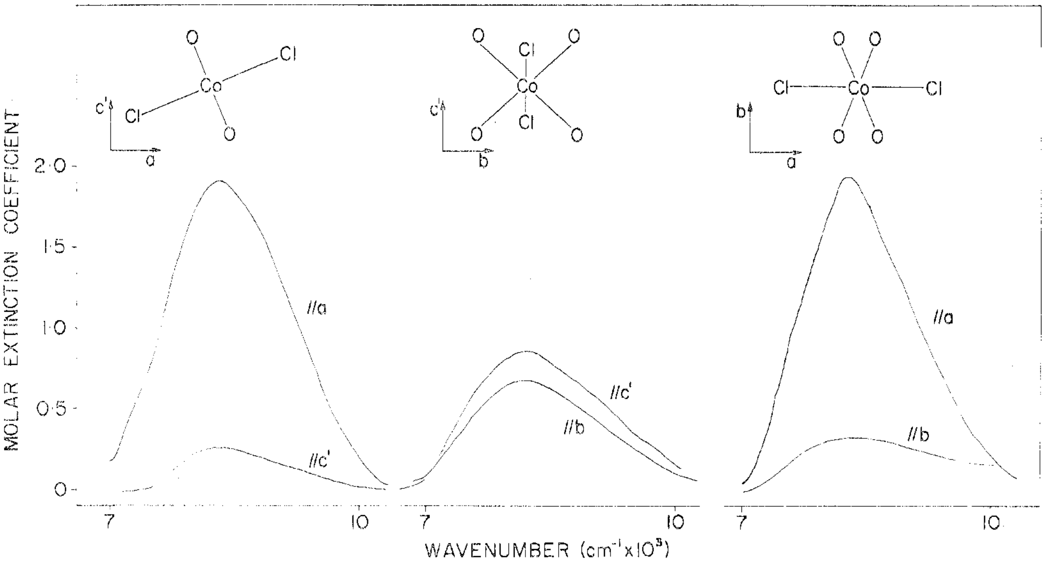

Figure 3. Polarized absorption spectra of $CoCl_2 \cdot 6H_2O$ in the near infrared region (10–40 K).

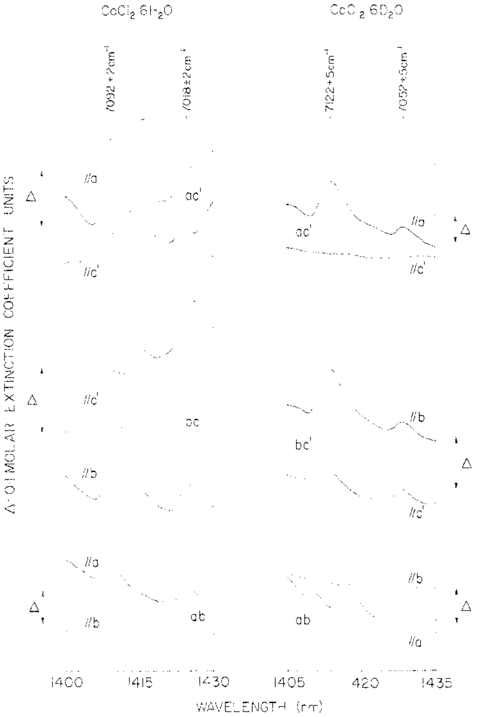

Figure 4. Fine structure on low-energy side of the near infrared bands in $CoCl_2 \cdot 6H_2O$ and $CoCl_2 \cdot 6D_2O$ (10-30 K).

(Table II) with the vibronic band lying at 8330 ± 60 cm^{-1}. In the *ac*' spectrum 16% of the relatively intense *z*-polarized band (Table II) is quite sufficient to shift the *c*'-polarized Franck–Condon maximum to an intermediate position at 8200 cm^{-1}. This is quite reasonable because we have made no allowance for possible dispersion of the extinction directions, the alignment being performed with visible light.

The $^4B_{2g}$ and $^4E_g{}^b$ states are then associated with the bands at 8060 and 8330 cm^{-1} which gives $|Dt| = 30 \pm 10$ cm^{-1}. Next we note from the selection rules for magnetic dipole transitions that *xy* polarization corresponds to either $^4A_{2g}{}^a \rightarrow {}^4E_g{}^b$ or $^4E_g{}^a \rightarrow {}^4B_{2g}$. The latter transition should also have a *z*-polarized component, approximately twice the *xy* polarization intensity, so that we conclude that the ground state is $^4A_{2g}{}^a$ (see paper I for a discussion of this point).

The Visible and Ultraviolet Regions. This region of the spectrum arises through electric dipole absorption and the room-temperature polarized absorption spectra for light incident normal to the *ab* face are shown in Figure 5. Observations with other faces show that the *b*- and *c*'-polarized spectra are very similar although the latter is somewhat weaker throughout the whole region.

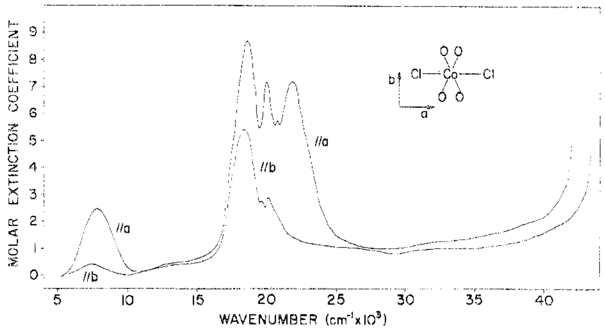

Figure 5. Polarized absorption spectrum of an *ab* face of $CoCl_2 \cdot 6H_2O$ (300 K).

Table III. Positions and Intensities of Absorptions in the Spin-Allowed Regions of the $CoCl_2 \cdot 6H_2O$ spectrum

	Oscillator strength[b]		
Position[a]	f_a	f_b	$f_{c'}$
8,060 ± 60 8,330 ± 60		See Table II	
11,500 ± 100	<0.2	2.0	<0.2
16,450 ± 100	0.25	0.7	0.7
17,800 ± 40	0.6	0.6	0.6
18,660 ± 40[c]	20		
18,410 ± 20 18,850 ± 40 [c]		18.5	13
22,250 ± 20	22	0.5	<0.5

[a] Franck–Condon maxima at 10 K (cm^{-1}). [b] Measured at 10 K in units of 10^{-6}. f_a, f_b, and $f_{c'}$ refer to the appropriate polarizations. [c] Two resolved maxima appear in *b* and *c*' polarizations but only one appears in *a* polarization.

Apart from the 11,500- and 25,800-cm^{-1} regions, which are considered separately below, the intensities of all bands decrease considerably on cooling the crystals, with the development of much fine structure in the 20,000–21,000-cm^{-1} region. Figure 6 shows the spectra for all three crystal axes, measured between 10 and 20 K.

The two strong bands resemble those of the tetragonal cobalt fluorides and they are assigned to transitions to $^4E_g{}^c$ and $^4A_{2g}{}^b$. Their centroids, in *a* polarization, are separated by about 3850

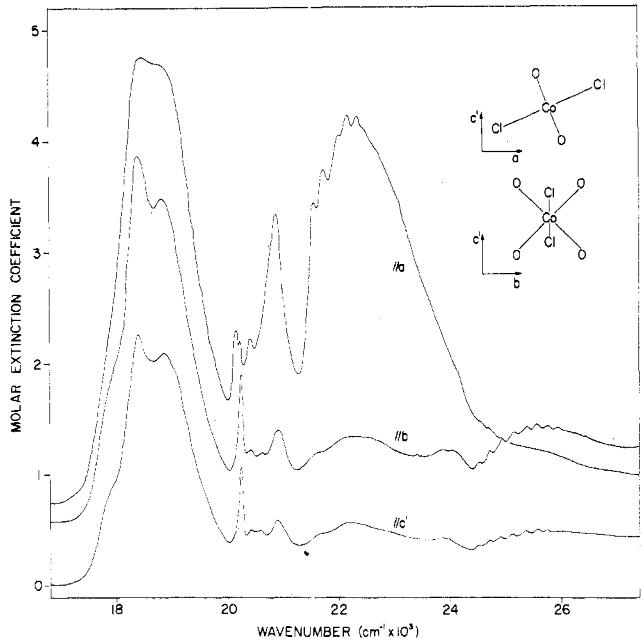

Figure 6. Polarized absorption spectra of $CoCl_2 \cdot 6H_2O$ in the visible region: *ac'*∥*a* (16 K); *bc'*∥*b* (10 K); *bc'*∥*c'* (10 K).

Table IV. Assignments of the Spin-Allowed Bands of the $CoCl_2 \cdot 6H_2O$ Spectrum

Position[a]	Assignment I	Position[a]	Assignment I
22,250 ± 20	$^4A_{2g}{}^b$	8,330 ± 60	$^4B_{2g}$
18,600 ± 40	$^4E_g{}^c$	8,060 ± 60	$^4E_g{}^b$
16,450 ± 100	$^4B_{1g}$	Ground state	$^4A_{2g}{}^a$

[a] Franck–Condon maxima at 10 K (cm^{-1}).

cm^{-1} and so a preliminary value of $|Ds|$ is set as 650 cm^{-1}. The experimental band positions and intensities of the main bands are given in Table III.

Crystal Field Parameters. The large value of *Ds* means that the ground state is governed by its sign. A positive value for *Ds* means that the ground state would be $^4E_g{}^a$ but this is contrary to the conclusion reached from an analysis of the near-infrared region and it is also contrary to expectations based on the relative positions of chloride and water in the spectrochemical series. A negative value for *Ds* leads to a $^4A_{2g}{}^a$ ground state and the assignments of the other quartet states are given in Table IV.

The separation between the Franck–Condon maxima of the $^4B_{1g}$ and $^4B_{2g}$ bands provides a well-defined value for 10*Dq* and we obtain $Dq = 810 \pm 15$ cm^{-1}. Calculations were then performed (see paper I for details) in order to obtain the best values for *Ds* and *Dt* from the separations between $^4E_g{}^b$ and $^4B_{1g}$ (for *Dt*) and $^4A_{2g}{}^b$ and $^4E_g{}^c$ (for *Ds*). The final set of crystal field parameters, $Dq = 810 \pm 15$ cm^{-1}, $Ds = -610 \pm 15$ cm^{-1}, and $Dt = 30 \pm 10$ cm^{-1}, along with the ^4P repulsion energy set at 12,500 cm^{-1} (85% of the free-ion value), gave an excellent fit to the observed spectrum, as can be seen from Figure 7.

There is a shoulder, near 17,800 cm^{-1} in all polarizations, which can be assigned to a set of doublet states arising from the ^2G term. With a value for the latter of 15,100 cm^{-1} (91% of the free ion value) we calculate that there are three states at 17,666 cm^{-1} (Γ_7), 17,900 cm^{-1} (Γ_7), and 17,870 cm^{-1} (Γ_6), with a total quartet character of 6%. This adequately explains the observed intensity of 3–4% of the intensity of the neighboring spin-allowed band.

Spectral Fine Structure. At low temperatures, as can be seen from Figure 6, the *a*-polarized band near 22,000 cm^{-1} displays vibrational fine structure, apparently a progression in a single mode of about 200 cm^{-1}. However the interval between successive bands varies from 160 to 240 cm^{-1} and it is likely that more than one vibration is involved.

The Raman spectrum of powdered $CoCl_2 \cdot 6H_2O$ has been reported by Adams and Lock[15] and it includes the three frequencies 183, 199, and 232 cm^{-1}. In order to assign the symmetry species of these vibrations we measured single-crystal Raman spectra at 30–40 K. Unfortunately a krypton plasma emission line at 15,222 cm^{-1} made it impossible to detect the 232-cm^{-1} vibration, but polarized measurements of the 199- and 183-cm^{-1} lines were made and they are shown in Figure 8. The polarization properties of these two lines indicate that the 183-cm^{-1} mode has a_g (C_{2h}) symmetry while the 199-cm^{-1} mode has b_g (C_{2h}) symmetry. We note next that Anantha-

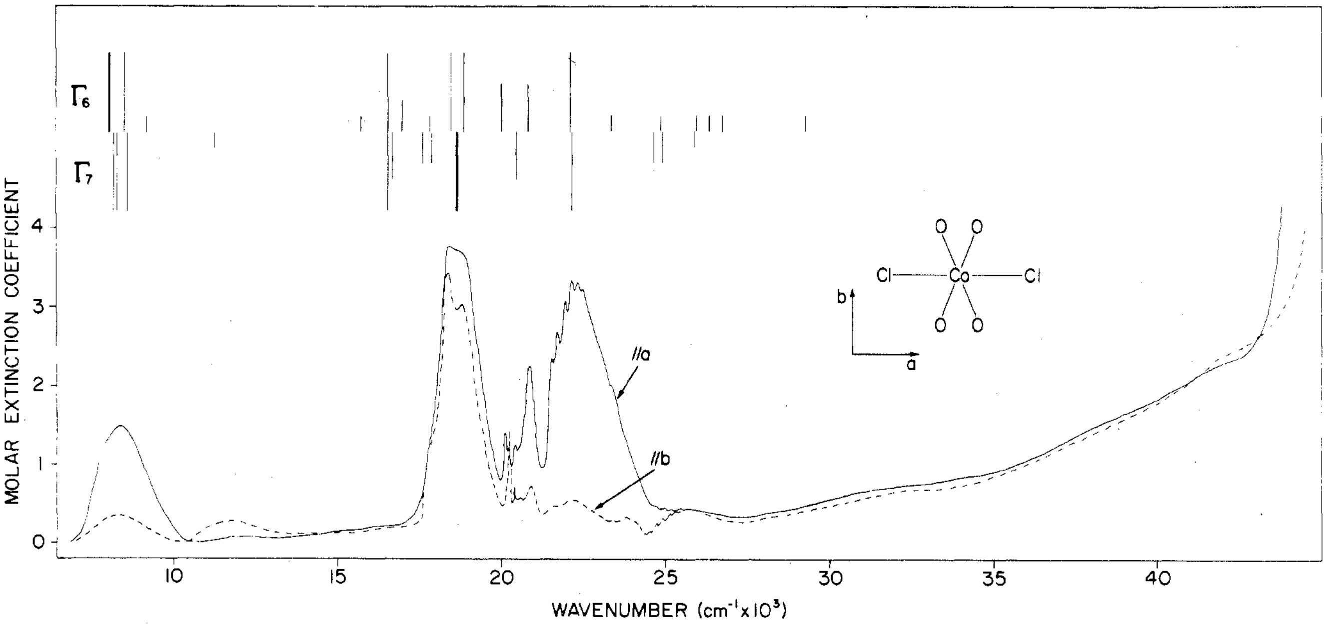

Figure 7. Polarized absorption spectrum of $CoCl_2 \cdot 6H_2O$ (*ab* face) together with an energy level scheme calculated with the parameters $Dq = 800$, $Ds = -610$, $Dt = 30$, and $\zeta = -490$. Electron repulsions: $^4P = 12{,}500$, $^2H = 18{,}500$, $^2G = 15{,}100$, $^2F = 30{,}000$, $^2P = 17{,}800$, $^2D = \begin{vmatrix} 41{,}100 & 10{,}500 \\ 10{,}500 & 24{,}600 \end{vmatrix}$ (all in cm^{-1}).

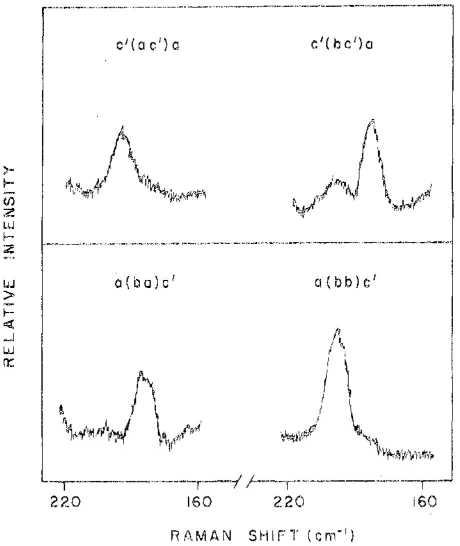

Figure 8. Raman shift spectra of $CoCl_2 \cdot 6H_2O$ (30–40 K).

narayanan and Danti[16] have made Raman studies of $K_2Co(SO_4)_2 \cdot 6H_2O$ and they reported a 212-cm^{-1} vibration which they assigned to the e_g fundamental of the octahedron. This mode will split into a_g and b_g in C_{2h} symmetry and it seems likely that the 183 and 199 cm^{-1} vibrations are the two components of the octahedral e_g fundamental. It seems probable therefore that one of the totally symmetric vibrations appearing in the electronic spectrum involves primarily a motion of the water molecules. If we examine the strong-field wave functions, *i.e.*

$$^4A_g{}^a\text{:}\quad (xy)(xz)^2(yz)^2(x^2-y^2)(z^2)$$

$$^4A_{2g}{}^b\text{:}\quad (xy)^2(xz)(yz)(x^2-y^2)^2(z^2)$$

we note that, as a result of the electronic transition, an electron is promoted to the $(x^2 - y^2)$ orbital and the resultant nuclear change should primarily involve a symmetrical relaxation of the water molecules. On the other hand, the transition to $^4E_g{}^c$ involves a promotion of the electron partly to $(x^2 - y^2)$ and partly to (z^2), so that the six ligands are involved and the mean displacement will be less. This probably explains the narrower bandwidth and the lack of resolved vibrational structure is most likely a result of overlapping progressions from the more complicated spin–orbit structure of this band.

Between the two spin-allowed bands in the visible region there are transitions to three states arising from the free-ion ^2P term. A number of relatively sharp lines are found in this region and there is a pronounced temperature dependence of the intensity of some of these lines. Figure 9 shows this region for light incident normal to the *ab* face. Two lines, shown by the arrows are apparently associated with the intense lines at 20,178 ± 5 cm^{-1} ($\|a$) and 20,272 ± 5 cm^{-1} ($\|b$). The separations from the intense lines are 130 ± 20 cm^{-1} and their intensities are qualitatively consistent with the ground state of these "hot" lines approximately 130 cm^{-1} above the ground state. We note that the presence of an electronic level about 130 cm^{-1} above the ground state is consistent with a $^4A_{2g}$ but not a ^4E_g assignment for the ground state.

The Anomalous Bands. There are bands in the absorption spectrum of $CoCl_2 \cdot 6H_2O$ which are anomalous because of the following properties. (1) They are strongly polarized along the *b* crystal axis, *i.e.*, along the *x* axis of the $CoCl_2(H_2O)_4$ complex. (2) Their intensities increase in a linear manner on cooling the crystal. (3) The bands appear at a lower energy in the spectrum of $CoCl_2 \cdot 6D_2O$, whereas the normal crystal field bands are not shifted.

In the usual mechanism for electric dipole absorption of light by a metal ion in a centrosymmetric site, the Laporte prohibition is removed by the perturbing effect of u vibrations and the important vibrations are assumed to be metal–ligand stretching modes. However, in the case of hydrates the water molecules have their own internal motions which can provide a noncentrosymmetric field at the metal ion. The three vibrations of the water molecule are well known,[17] *i.e.*, the symmetrical OH (OD) bending mode at 1595 (1179) cm^{-1}, the symmetrical OH stretching mode at 3652 (2666) cm^{-1}, and the asymmetrical OH stretching mode at 3756 (2789) cm^{-1}.

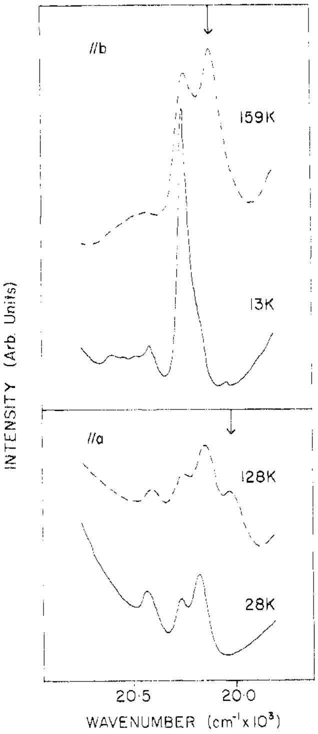

Figure 9. Temperature dependence in the ^2P region of the spectrum of $CoCl_2 \cdot 6H_2O$ (*ab* face).

The possibility of the excitation of water vibrations, coupled to an electronic excitation, was suggested by Piper and Koertge[18] to explain some very weak structure in the absorption spectra of various hydrated nickel crystals. More recently, a study of the MCD spectrum of $Ni(BrO_3)_2 \cdot 6H_2O$[19] showed a set of weak lines about 3000 cm^{-1} to higher energy of the $^3A_{2g} \rightarrow {}^3T_{1g}{}^a$ band, which were assigned to a combination of a water vibration and metal–water vibrations. In the case of $CoCl_2 \cdot 6H_2O$ studied here, the known locations of the protons[12] allow a definitive assignment to be made.

The absorption spectra of $CoCl_2 \cdot 6H_2O$ (*ab* face) and $CoCl_2 \cdot 6D_2O$ ($\|b$, *ab* face), taken at 10 K, are shown in Figure 10 for the region 20,000–27,000 cm^{-1}. The temperature dependence of the region 23,000–27,000 cm^{-1}, for $CoCl_2 \cdot 6H_2O$, is shown in Figure 11.

From Figure 10 we note the two band groups A and B. The first corresponds to transitions to a group of doublet states arising from ^2P, while the second is associated with the excited state $^4A_{2g}$, nearly completely polarized $\|a$.

Coupled to A and B are the anomalous band groups A' and B'. In the spectrum of $CoCl_2 \cdot 6H_2O$ A' and B' occur approximately 3200 cm^{-1} to higher energy of A and B, respectively, while in the spectrum of $CoCl_2 \cdot 6D_2O$ the separation is approximately 2340 cm^{-1}. (These separations are more accurately defined from comparisons of the vibrational substructure (a, b, ..., g; a', b', ..., g').) These values are both 88% of the free molecule energies of the symmetrical stretching mode in each case.[17]

Bands B and B' have very similar vibrational structure but

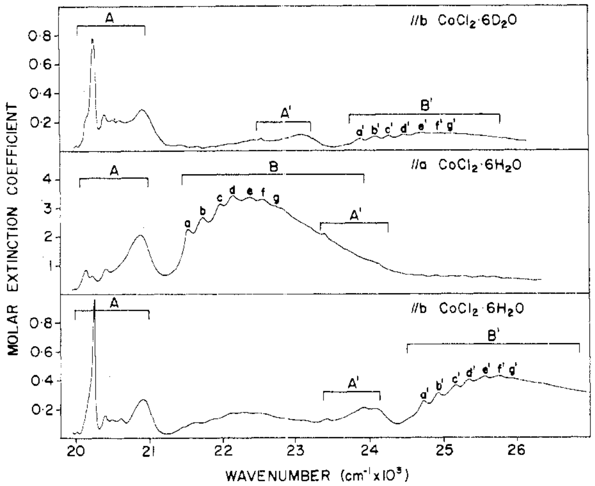

Figure 10. Absorption spectra of $CoCl_2 \cdot 6H_2O$ and $CoCl_2 \cdot 6D_2O$ in the visible region showing the anomalous crystal field bands.

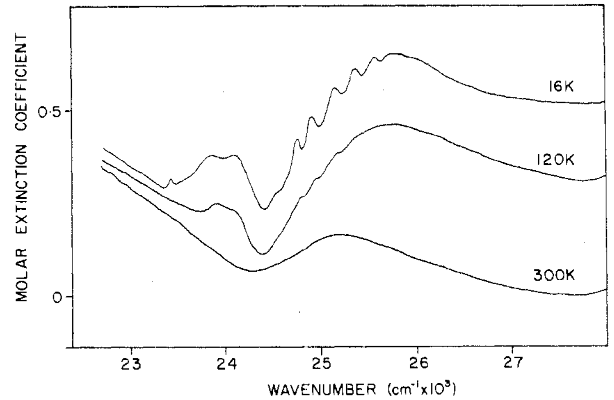

Figure 11. Temperature dependence of the 23,000–27,000-cm^{-1} region of the absorption spectrum of $CoCl_2 \cdot 6H_2O$ (*ab* face, ‖*b*).

they have opposite polarization. We are able to understand this feature from a consideration of the nature of the water vibrations. There are four water molecules in the complex unit, so that each water fundamental gives rise to four coupled motions transforming as a_g, b_g, a_u, and b_u of the site group C_{2h}. The C_2 axis of the water molecule lies close to the direction of the crystal *b* axis (see Figure 1, *ab* face) and it is easy to see that the a_u component carries a large dipole moment, parallel to *b*, while the b_u component has a much smaller dipole moment perpendicular to *b* (close to the $Co(H_2O)_4$ plane). Similarly it can be seen that the asymmetrical OH(D) stretch has a much larger amount for the b_u component than for a_u. As the ground and excited electronic states for band B have the same symmetry (^4B_g in C_{2h}), the observed *b* polarization of band B' is consistent with the involvement of the symmetric stretching mode as the perturbing vibration ($B_g \times B_g \times a_u \equiv A_u$).

Although the symmetrical OH stretching mode is primarily a motion of the hydrogen atoms, the oxygen atom is also involved[17] so that the bonding between the cobalt ion and the water molecules is modulated by the vibration. Therefore, when D_2O is considered, the amplitude of the oxygen motion should be nearly twice that of H_2O and we would expect a greater perturbing effect. However, as can be seen from Figure 10, the symmetrical OD stretching mode is less effective than the OH mode and we must look to another mechanism. It is not our purpose to consider this problem quantitatively here, but it seems likely that the effectiveness of the symmetrical stretching mode is related to the magnitude of its dipole moment and the effect this has in providing an asymmetric electric (polarizing) field for the cobalt d electrons.

The assignment of the anomalous crystal field bands in the region 20,000–27,000 cm^{-1} to OH-induced transitions raises the possibility that other electronic transitions might also be involved in this mechanism. We note that the anomalous band near 11,500 cm^{-1} is approximately 3500 cm^{-1} higher in energy than the $^4A_{2g}{}^a \rightarrow {}^4E_g{}^b$, $^4B_{2g}$ transition. It is also strongly polarized parallel to the *b* crystal axis and, if we assume that the symmetrical OH stretching mode is involved, then we conclude that the excited state cannot be $^4B_{2g}$ (D_{4h}). It must be the B_g (C_{2h}) component of $^4E_g{}^b$. There is no evidence from the 20,000–27,000-cm^{-1} spectral region to suggest that the OH mode plays any role in promoting the transition $^4A_{2g} \rightarrow {}^4E_g{}^c$ and we conclude that its effectiveness is confined to three groups of states, ^4B_g from $^4E_g{}^b$, $^4A_{2g}{}^b$ and the doublet states from ^2P. The reason for this must await further theoretical investigation, outside the scope of the present paper.

We note finally that although the magnitude of the intensity stealing is not large (approximately 2×10^{-6} oscillator strength for the 11,500- and 25,800-cm^{-1} bands) it is comparable to the usual cobalt–ligand mechanism operating in the near-infrared region ($^4B_{2g}$ and $^4E_g{}^b$ excited states).

Conclusion

It appears from our analysis that a complete assignment of the spin-allowed bands in the spectrum of $CoCl_2 \cdot 6H_2O$ is possible using the tetragonal weak-field matrices for $d^{3,7}$. The optimum "mean" values of the parameters are $Dq = 810 \pm 15$ cm^{-1}, $Ds = -640 \pm 15$ cm^{-1} and $Dt = 30 \pm 10$ cm^{-1}. The value of Dq lies between Dq_{Cl} and Dq_{H_2O}, very close to an "average" value, *i.e.*, $^2/_3 Dq_{H_2O} + {}^1/_3 Dq_{Cl} = 830$ cm^{-1}. This is probably fortuitous as there is no physical basis for assuming that each ligand will exert the same crystal field in the cubic and tetragonal complexes. Also, Dt is much smaller than expected from the point charge model (~120 cm^{-1}) and it is probable that the effective values of Dq_{H_2O} and Dq_{Cl} are somewhat closer to each other. The negative value for Ds is incompatible with the point charge model and another model, such as that introduced by Donini, *et al.*,[20] should be considered for this type of complex.

Registry No. $CoCl_2 \cdot 6H_2O$, 36120-14-6; $CoCl_2 \cdot 6D_2O$, 52873-78-6.

References and Notes

(1) J. Ferguson and T. E. Wood, following paper.
(2) T. Haseda and E. Kanda, *J. Phys. Soc. Jap.*, **12**, 1051 (1957).
(3) (a) T. Haseda, *J. Phys. Soc. Jap.*, **15**, 483 (1960); (b) N. Uryu, J. Skalyo, and S. A. Friedberg, *Phys. Rev.*, **144**, 689 (1966).
(4) I. Kimura and N. Uryu, *J. Chem. Phys.*, **45**, 4368 (1966).
(5) B. N. Figgis, M. Gerloch, F. E. Mabbs, and G. A. Webb, *J. Chem. Soc. A*, 2086 (1968).
(6) M. Gerloch, P. N. Quested, and R. C. Slade, *J. Chem. Soc. A*, 3741 (1971).
(7) J. Gielessen, *Ann. Phys. (Leipzig)*, **22**, 537 (1935).
(8) R. Pappalardo, *Phil. Mag.*, **4**, 219 (1959).
(9) J. Ferguson, *J. Chem. Phys.*, **32**, 533 (1960).
(10) J. Mizuno, *J. Phys. Soc. Jap.*, **15**, 1412 (1960).
(11) J. Mizuno, K. Ukei, and T. Sugawara, *J. Phys. Soc. Jap.*, **14**, 383 (1959).
(12) Z. M. el Saffar, *J. Phys. Soc. Jap.*, **17**, 1334 (1962).
(13) J. Ferguson, H. J. Guggenheim, and D. L. Wood, *J. Chem. Phys.*, **53**, 1613 (1970).
(14) T. R. Gilson and P. J. Hendra, "Laser Raman Spectroscopy," Wiley-Interscience, London, 1970.
(15) D. M. Adams and P. J. Lock, *J. Chem. Soc. A*, 2801 (1971).
(16) U. Ananthanarayanan and A. Denti, *J. Mol. Spectrosc.*, **20**, 88 (1966).
(17) G. Herzberg, "Infrared and Raman Spectra," Van Nostrand, New York, N. Y., 1945.
(18) T. S. Piper and N. Koertge, *J. Chem. Phys.*, **32**, 559 (1960).
(19) M. J. Harding, S. F. Mason, D. J. Robbins, and A. J. Thomson, *J. Chem. Soc. A*, 3047 (1971).
(20) J. C. Donini, B. R. Hollebone, and A. B. P. Lever, *J. Amer. Chem. Soc.*, **93**, 6455 (1971).